

Rethinking the positive role of cluster structure in complex networks for link prediction tasks

Shanfan Zhang, Wenjiao Zhang, Zhan Bu

Abstract—Clustering is a fundamental problem in network analysis that finds closely connected groups of nodes and separates them from other nodes in the graph, while link prediction is to predict whether two nodes in a network are likely to have a link. The definition of both naturally determines that clustering must play a positive role in obtaining accurate link prediction tasks. Yet researchers have long ignored or used inappropriate ways to undermine this positive relationship. In this article, We construct a simple but efficient clustering-driven link prediction framework (*ClusterLP*), with the goal of directly exploiting the cluster structures to obtain connections between nodes as accurately as possible in both undirected graphs and directed graphs. Specifically, we propose that it is easier to establish links between nodes with similar representation vectors and cluster tendencies in undirected graphs, while nodes in a directed graphs can more easily point to nodes similar to their representation vectors and have greater influence in their own cluster. We customized the implementation of *ClusterLP* for undirected and directed graphs, respectively, and the experimental results using multiple real-world networks on the link prediction task showed that our models is highly competitive with existing baseline models. The code implementation of *ClusterLP* and baselines we use are available at <https://github.com/ZINUX1998/ClusterLP>.

Index Terms—cluster-aware graph neural networks, cluster structure, link prediction, network reconstruction.

I. INTRODUCTION

LINK prediction has gained in popularity in the past decade, because of the increasing prominence of network data. Its goal is to infer missing links or predict future links based on currently observed networks. Meanwhile, it's widely used in a variety of real-world applications, from product recommendations in social networks to interaction discovery in biology, from knowledge graph to graph structure capture. Link prediction algorithms represent an important family of tools for studying the underlying structure of networks. Despite its wide presence, most existing link prediction algorithms are inherently limited to lower-order structures (i.e., nodes and edges) and undirected networks. They analyze network topology information to predict future links. The most intuitive assumption of these methods is that the more similar the two nodes are, the more likely they are to have links. Based on this assumption, how to describe and calculate the similarity between nodes become a basic problem of link prediction.

Existing link prediction approaches can be roughly divided into three categories: topological similarity approaches, probabilistic approaches, classification-based approaches, and similarity-popularity approaches. Topological similarity-based methods do not require building a model of the network; they measure the score or distance between each pair of nodes in the network. This score is then used to estimate the possibility that the two corresponding nodes will form an edge. Probabilistic methods are usually based on Markov chains and Bayesian networks. They build a model for the whole network, which is then used to estimate the connection probability between disconnected pairs of nodes. Classification-based approaches predict links by training a classifier to discriminate between connected and disconnected couples using various topological features. Similarity-popularity methods assume that the connection between nodes is driven by two factors: popularity, which is an intrinsic property of the node, and similarity between nodes. Although many efforts have been devoted to the link prediction, two open problems are still poorly understood, which are summarized as follows:

- 1) How to combine high-order structure with link prediction. High-order structure information refers to some local connections in the network (the number of nodes is greater than or equal to 3), such as triangles, star topological structures, and so on. Unfortunately, most of the previous works focus on the microscopic architectures formed among nodes, which means that they concentrate on individual node and aim to output a vector representation for each node in the graph, such that two nodes “close” on the graph have similar vector representations in the low-dimensional space.
- 2) For directed networks, link prediction requires predicting not only the presence of links but also the direction of links. We can't judge the direction of a link based on similarity alone, so how to predict the direction of links is another challenge in link prediction. In undirected networks, the link prediction task usually considers the similarity of nodes, but in directed networks, because of the directivity of links, it is not enough to consider only the similarity of nodes. We need to find a prediction method that can predict the direction of links.

Numerous literatures (e.g., ([35])) show that complex networks in the real world can be naturally divided into multiple cluster structures, which can characterize the local aggregation characteristics and reflect the distribution inhomogeneity of connected edges in the network. Take the World Wide Web as an example, through hyperlinked pages, the pages of the same

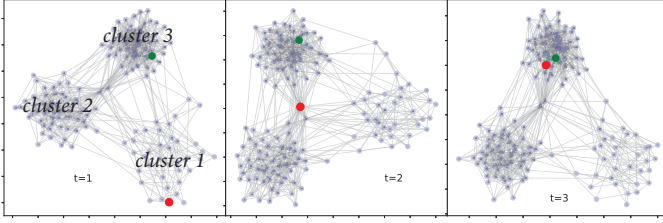


Fig. 1: Evolution of simulated graph topology through time [1]. There are three distinct cluster-like structures in the network, with the nodes and edges contained in each cluster constantly evolving over time.

community have similar topics. Based on this perception, deep clustering methods aim to combine the deep representation learning with the clustering objective. For example, by introducing the loss function of K-means clustering results in the autoencoder, ([15]) proposes a deep clustering network that can learn a "K-means-friendly" data representation. Similarly, in order to improve the cluster cohesion, deep embedding clustering([12]) brings the representations learned by the autoencoder closer to the cluster center by designing a KL-divergence loss. Improved deep embedding clustering([13]) adds a reconstruction loss to the objective of DEC as a constraint to help autoencoder learn a better data representation. Variational deep embedding([16]) achieves better clustering results using a deep variational autoencoder that is capable of joint modeling of both the data generation process and clustering. However, the cluster structure information in these methods only serves as auxiliary information to adjust the obtained node representation, while has no useful utility in obtaining the representation vectors that can accurately reflect the connection relationship between nodes.

Take Fig.1 as an example, at different moments, red node gradually shifts from one cluster to another, with adjacent nodes varying greatly, while green node is always in the same cluster, by comparison, with little change at the three moments. This phenomenon has inspired us to perhaps use the cluster structures in the network to guide the acquisition of node embeddings that can more accurately reflect the structure of the real network topology, specifically, links likely between nodes in the same cluster than nodes belonging to different clusters.

Based on the above analysis, we propose a new link prediction framework combining the cluster structure in the network. The important ideas are: 1) calculate the *first-order proximity* between nodes using the representation vector of the nodes; 2) capture the *cluster-level proximity* between nodes using the tendency of nodes to clusters in the network; 3) the probability of forming links between nodes is the result of *first-order proximity* and *cluster-level proximity*. By interactively updating the node representation vectors and cluster centroids, the resulting link formation probability will eventually converge to an ideal state that reflects the true network topology as much as possible. In summary, the contributions of this paper are listed as follows:

- 1) We explore a novel connection formation mechanism

that combines not only the *first-order proximity* of nodes in the representation space but also innovatively combines *cluster-level proximity* to determine the underlying connection probability of any two nodes. Compared with the existing models, our proposed ClusterLP framework is more interpretable since the resulted distribution of nodes in the representation space is consistent with true network topology.

- 2) To extend the receptive fields of nodes and the propagation range of information, we introduce cluster centroids. Instead of using cluster structure as an indicator to judge the quality of obtained node representation vectors, we explicitly use cluster centroids to guide the acquisition of node representation vectors. Compared with existing node embedding models, the proposed model can effectively capture the global information of the network, resulting into better nodes representation.
- 3) We have customized the implementation of our *ClusterLP* framework for undirected and directed graphs, respectively, and performed extensive evaluation on multiple real-world datasets. Experimental results show that our models are sufficient to compete effectively with the state-of-the-art baseline models, which validates the feasibility of *ClusterLP*.

The rest of this paper is organized as follows: Section II contains the related works; Section III introduces the problem definition of this paper; Section IV introduces some preliminaries before presenting our method; Section V introduces our link prediction method based on clustering; Section VI shows the experimental results. Section VII concludes our works in link prediction and points out the future works.

II. RELATED WORKS

Link prediction is essential to dig out the reasons and driving forces for the connections of nodes. This section will first present link prediction methods for undirected networks, many of which can be used or adapted to directed networks but do not exploit the asymmetric nature of the relationships; then some link prediction methods specifically designed for directed networks will be reviewed; finally, we will highlight some pioneering work on obtaining or optimizing node representations using cluster structures, which will be our main contrast tools.

A. Link prediction in undirected networks

1) *Topological similarity methods*: Traditional topological similaritybased methods predict the link probability by mining the topology structure in the network. They come up with metrics based on topological similarity, and always follow the principle that the greater such metrics, the greater the probability of linking.

Common Neighbor (CN) [28] is the most widely used adjacency relations-based link prediction method with the advantages of low computational complexity and strong interpretability, which follows the strategy that if there are more co-neighbors between two nodes, the more likely there is a link between them. Jaccard Coefficient (JC) [29] improves

CN by considering the total number of neighbors, and is in fact a standardized version of CN. Adamic and Adar (AA) [30] improves the prediction accuracy by exploiting the degree to distinguish between the contributions of different common neighbors, in which the nodes with fewer neighbors are assigned higher scores. Works exploiting *second-order proximity* between nodes to embed networks can also be included in such models. For example, to embed the networks by preserving both the first-order and second-order proximity, [21] trains the *LINE* model which preserves the first-order proximity and second-order proximity separately and then concatenate the embeddings trained by the two methods for each vertex.

DeepWalk [36] extended the idea of *Skip-Gram* to model network, which is convert to a corpus of node sequences by performing truncated random walks. *Node2vec* [20] introducing a biased random walk procedure which combines BFS style and DFS style neighborhood exploration.

2) *Probabilistic methods*: Probabilistic approaches assume that the network has a known structure and build a model to fit the structure by estimating its parameters using statistical methods, the trained model is finally used to estimate the probability of absent edges. The Hierarchical Random Graph model [32] is a typical probabilistic model that utilizes the fact that many real networks exhibit a hierarchical structure, specifically, a) nodes with a high degree have a lower clustering coefficient than low-degree nodes; b) high-degree nodes weakly connect highly clustered nodes within isolated communities. Based on the above observations, the model proposes that a dendrogram where each leaf represents a node in the network, and each internal node represents a cluster can be used to characterize a network. Each internal node of the dendrogram is associated with the probability that a link exists between any of its children and the probability that two nodes are connected can then be computed by finding their lowest common ancestor.

3) *Classification-based approaches*: Link prediction can be seen as a classification problem with two classes: positive class represents connected pairs of nodes, whereas the negative class consists of disconnected couples. Hasan et al. [33] used, a) local features such as the short distance between two nodes; b) aggregated features such as a sum of neighbors; c) semantic features such as the number of matching keywords, to build a classifier model that helps predict author collaboration and evaluated their approach on two co-authorship networks. They assessed each feature visually by comparing the densities of the classes and then using well-defined feature ranking methods, and experimentally conclude that semantic similarity helps to improve the accuracy of link prediction.

4) *Similarity-popularity methods*: Those methods ascribe network topology to the similarity between nodes and their popularity, working under the assumption that the more similar and popular the two nodes are, the higher their connection probability.

The Hidden Metric Space Model (*HMSM*) proposed in [34] assumes the existence of a hidden metric space that underlies the network and governs the similarity between nodes. The probability of connecting two nodes in an undirected network based on *HMSM* is defined as follows:

$$r_{ij} = \left(1 + \frac{d_{ij}}{\phi(\kappa_i, \kappa_j)}\right)^{-\alpha} \quad (1)$$

where d_{ij} is the distance between nodes i and j , κ_i and κ_j denote their expected degrees, and the characteristic distance scale $\phi(\kappa_i, \kappa_j) \approx \kappa_i \kappa_j$. The hyperparameter α represents the influence of the hidden metric space on the observed topology, and setting α to a large value will lead to a strong clustering in the network. The connection probability $\kappa_i \kappa_j$ increases when, a) the distance d_{ij} becomes small, i.e., similar nodes have a high probability to connect; b) $\kappa_i \kappa_j$ becomes large, reflected in real networks where popular nodes (characterized by high degrees) tend to connect to many other nodes.

B. Link prediction in directed networks

1) *Similarity measures based on in-degree and out-degree (neighborhood direction)*: To solve the link prediction problem in directed networks, approaches [7], [6] usually firstly decompose the target directed network into the in-degree and out-degree networks, and then apply the link prediction technologies such as GCN to each network independently. However, this intuitive strategy cannot fully preserve the network structure information in the process of link prediction[22].

2) *Motif Based methods*: Motifs are small, connected, non-isomorphic induced subnetworks in networks and each motif represents a topological pattern of interconnection between k nodes. Benson et al. [25] first proposed that there are totally 13 motifs with $k = 3$ nodes in directed networks, and indicated that more attention should be paid to the local information in the process of link prediction. Since then, Aghabozorgi et al. [27] proposed a link prediction measure which combined the common neighbor similarity and the triad similarity obtained by counting the number of common participating motifs between nodes; Ghorbanzadeh et al. [26] proposed a link prediction method based on the number of common neighbors and two specific motifs called hub and authority.

3) *Graph neural network Based methods*: To extend GAE to directed networks, Salha [5] proposed a new gravity-inspired decoder named *Gravity-GAE*, which follows a strategy that linking probability is determined by the similarity of nodes, and links always lead from the high mass to the low mass. Specifically, the probability of node i connecting to node j in a directed graph is defined as

$$\hat{A}_{ij} = \sigma(\log a_{i \rightarrow j}) = \sigma(\tilde{m}_j - \lambda \log \|z_i - z_j\|_2^2) \quad (2)$$

where \tilde{m}_j is the mass of node j , $\|z_i - z_j\|_2^2$ denotes the distance between of the two nodes, additional parameter λ is introduced to improve the flexibility of the decoder, $\sigma(\cdot)$ is the activation function, \hat{A}_{ij} equals 1 if $\log a_{i \rightarrow j}$ is greater than 0.5, and 0 otherwise.

C. Cluster-related node representation models

Most existing unsupervised methods promote similar representations between topologically close nodes, however it has been shown that utilizing additional graph-level information,

e.g., information shared between all nodes, can encourage representation attention to the global properties of the graph, which greatly improves their quality.

Motivated by the phenomenon that significantly more structures can be captured in most graphs, e.g., nodes tend to belong to (multiple) clusters representing structurally similar nodes, *GIC* [11] seeks to additionally capture cluster-level information content. These clusters are computed by a differentiable K-means method and are jointly optimized by maximizing the mutual information between nodes of the same clusters.

CAGNN [24] alternates between node representation learning and clustering. Specifically, the pipeline of the model contains three phases, 1) obtain node embeddings using graph neural networks (GNN); 2) perform clustering and use the cluster labels as the self-supervisory signals; 3) use a novel cluster-aware topology refining mechanism which reduces inter-cluster edges and strengthens intra-class connections to mitigate the impact of noisy edges.

Wilder et al. [23] proposed *CLUSTERNET* system merges two differentiable components into a system that is trained end-to-end. The first component uses a graph embedding layer such as *GCNs*, to embed the nodes of the graph into R^p using the training set A^{train} and any node features. Next, a layer that implements a differentiable version of K-means clustering is used to produce a soft assignment of the nodes to clusters, along with the cluster centers in embedding space. This algorithmic structure can be fine-tuned to specific problems by training the first component, which produces the embeddings, so that the learned representations induce clusterings with high objective value for the underlying downstream optimization task.

III. THE PROPOSED METHOD

In this section, we begin with some preliminaries and formally define the link prediction problem in networks; then, we describe our proposed *ClusterLP* framework in detail; finally, we design two models ULP and LP for the undirected graph and directed graph link prediction task, respectively, and analyze their relationship with existing models. The main symbols used in this paper are listed in Table I.

A. Preliminaries

In practice, information networks can be either directed (e.g., citation networks) or undirected (e.g., social network of users in Facebook). The weights of the edges can be either binary or take any real value. Note that while negative edge weights are possible, in this study we only consider nonnegative weights. For example, in citation networks and social networks, w_{ij} takes binary values; in co-occurrence networks between different objects, w_{ij} can take any nonnegative value. The weights of the edges in some networks may diverge as some objects co-occur many times while others may just co-occur a few times.

Embedding an information network into a low-dimensional space is useful in a variety of applications. To conduct the embedding, the network structures must be preserved. The first intuition is that the local network structure, i.e., the local

TABLE I: Notations used throughout this paper

Notation	Description
$\mathcal{G} = (\mathcal{V}, \mathbf{A})$	the input graph
\mathcal{V}	the set of vertices
N	the number of nodes
$\mathbf{A} \in \mathbb{R}^{N \times N}$	the adjacency matrix of graph \mathcal{G}
v_i	the vertex with index i
\mathcal{E}	the set of edges
e_{ij}	the directed link from v_i to v_j
\mathcal{E}_{train}	the training set
\mathcal{E}_{test}	the test set
$\mathbf{A}_{train} = \{\mathbf{A}_{ij} \mid e_{ij} \in \mathcal{E}_{train}\}$	real labels of the training set
$\mathbf{A}_{test} = \{\mathbf{A}_{ij} \mid e_{ij} \in \mathcal{E}_{test}\}$	real labels of the test set
d	dimensions of the presentation space
\mathcal{K}	the number of clusters
$\mathbf{H} \in \mathbb{R}^{N \times d}$	the output embedding matrix
$\mathbf{H}_i \in \mathbb{R}^d$	the embedding of node v_i
$\mathbf{H}^{(t)}$	the output embedding of the t -th update
$\mathbf{D} \in \mathbb{R}^{N \times N}$	the first-order proximity of nodes
$\mathbf{U} \in \mathbb{R}^{\mathcal{K} \times d}$	the cluster centroids
$\mathbf{U}^{(t)}$	the cluster centroids of the t -th update
$\mathbf{T} \in \mathbb{R}^{N \times \mathcal{K}}$	the cluster-assignment matrix
$\mathbf{C} \in \mathbb{R}^{N \times N}$	the cluster-level proximity of nodes
$\mathbf{U}_k \in \mathbb{R}^d$	the centroid of cluster k
\mathbf{T}_{ik}	the tendency of node v_i to \mathbf{U}_k
$\mathbf{T}_i = [\mathbf{T}_{i1}, \mathbf{T}_{i2}, \dots, \mathbf{T}_{i\mathcal{K}}]$	the cluster assignment of v_i
$\mathbf{P} \in \mathbb{R}^{N \times N}$	link probability between nodes
p_{ij}	probability of a directed link from v_i to v_j

pairwise proximity between the vertices, must be preserved. We define the local network structures as the *first-order proximity* between the vertices:

Definition 1. (First-order Proximity) The *first-order proximity* in a network is the local pairwise proximity between two vertices. For each pair of vertices linked by an edge (v_i, v_j) , the weight on that edge, w_{ij} , indicates the first-order proximity between v_i and v_j . If no edge is observed between v_i and v_j , their *first-order proximity* is 0.

The *first-order proximity* usually implies the similarity of two nodes in a real-world network. For example, people who are friends with each other in a social network tend to share similar interests; pages linking to each other in World Wide Web tend to talk about similar topics. Because of this importance, many existing graph embedding algorithms such as *IsoMap*, *LLE*, *Laplacian eigenmap*, and *graph factorization* have the objective to preserve the *first-order proximity*.

However, in a real world information network, the links observed are only a small proportion, with many others missing. A pair of nodes on a missing link has a zero first-order proximity, even though they are intrinsically very similar to each other. Therefore, *first-order proximity* alone is not sufficient for preserving the network structures, and it is important to seek an alternative notion of proximity that addresses the problem of sparsity.

In order to solve this problem, *LINE* proposed the concept of *second-order similarity* between nodes based on the fact that vertices sharing similar neighbors tend to be similar to

each other.

Definition 2. (Second-order Proximity) The *second-order proximity* between a pair of vertices (v_i, v_j) in a network is the similarity between their neighborhood network structures. Mathematically, let $p_{v_i} = (w_{v_i,1}, \dots, w_{v_i,|\mathcal{V}|})$ denote the *first-order proximity* of v_i with all the other vertices, then the *second-order proximity* between v_i and v_j is determined by the similarity between p_{v_i} and p_{v_j} . If no vertex is linked from/to both v_i and v_j , the *second-order proximity* between v_i and v_j is 0.

While *second-order proximity* works well in many cases, we point out that it only considers the relationship between nodes with a minimum distance of 2 and can not capture the global information of the network like a stacked GCN layer, i.e., it does not overcome the drawback of a small receptive field as similar to *first-order proximity*.

Another natural intuition is that vertices in the same cluster tend to be similar to each other. For example, in social networks, people in the same social group often have similar interests, thus becoming friends; in citation networks, a node (article) is more willing to quote articles in the same research field. We therefore define the *cluster-level proximity*, which complements the *first-order proximity* and preserves the network structure.

Definition 3. (cluster-level proximity) The *cluster-level proximity* between a pair of vertices (v_i, v_j) in a network is the similarity between their tendencies toward the clusters present in the network. Mathematically, if t_i and t_j represent the cluster assignment of nodes v_i and v_j respectively, then the *cluster-level proximity* between v_i and v_j is determined by the similarity between t_i and t_j . If v_i and v_j are in the same cluster, the *cluster-level similarity* between them is high, otherwise it will be close to 0.

cluster-level proximity can be seen as a generalized version of *second-order proximity*, that is, the common neighbors between nodes are relaxed into communities, which brings the nodes in the network to a global perspective, and perfectly overcomes *second-order proximity*'s defects.

B. Problem Definition

Consider a graph $\mathcal{G} = \langle \mathcal{V}, \mathbf{A} \rangle$ with N nodes, where $\mathcal{V} = (v_1, v_2, \dots, v_n)$ represents a set of nodes and $\mathcal{E} = \{e_{ij} \mid v_i, v_j \in \mathcal{V}\}$ represents a set of edges where the nodes $v_i, v_j \in \mathcal{V}$ are connected. The adjacency matrix $\mathbf{A} \in \mathbb{R}^{N \times N}$ is defined by $\mathbf{A}_{ij} = 1$ if $e_{ij} \in \mathcal{E}$ and 0 otherwise. In an undirected graph, if \mathbf{A}_{ij} is equal to 1, \mathbf{A}_{ji} must also be equal to 1, namely, the relationship between v_i and v_j is equal and bidirectional, while in a directed graph, the relationship between \mathbf{A}_{ij} and \mathbf{A}_{ji} is uncertain, namely, the relationship between nodes v_i and v_j is unequal and one-way. From the definition, modeling the relationship between nodes in a directed graph will be much more difficult than that in undirected graphs, given the need to calculate not only the probability of forming edges between nodes, but also the direction of the edges.

As an important topic of graph data mining, link prediction is intended to predict the possibility of future links between

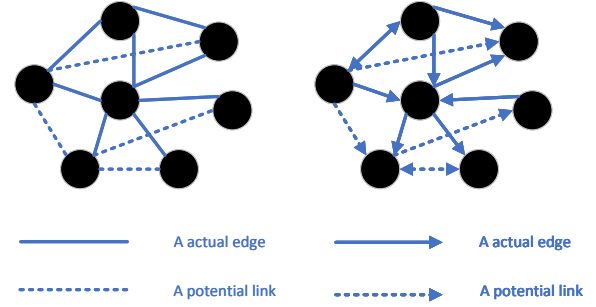


Fig. 2: Link prediction in undirected networks(left) and directed networks(right).

any two nodes in the network by analyzing existing network information. Fig.2 shows the differences of link prediction in undirected networks and directed networks. The link prediction in the directed networks need to predict the potential links in the network and give the link direction according to the topology information and attribute information in the networks. We usually hide some links of the network as input, and then make link prediction according to the network. The closer the predicted network is to the original network, the better the link prediction effect will be. With the above notions, link prediction in networks can be formally defined as follows:

Problem Formulation. Link Prediction in Networks

Input: The network $\mathcal{G} = \langle \mathcal{V}, \mathbf{A} \rangle$. All node pairs in \mathcal{G} are divided into two disjoint parts, which are the training set denoted by \mathcal{E}_{train} and the test set denoted by \mathcal{E}_{test} . Only the links contained in \mathcal{E}_{train} are used to train the prediction model.

Output: The reconstructed network with node pair set \mathbf{P} .

C. Methodology

Our proposed solution for the link prediction problem is shown in Fig.3. Concretely, we assume that the number of clusters \mathcal{K} in the network is already known (as a hyper-parameter of the model), *ClusterLP* will randomly assign a representation vector \mathbf{H}_i to each node v_i in the network and $u_j \in \mathbb{R}^d$ to the centroid of each cluster j at the initial moment. *ClusterLP* will be divided in two stages to train the output embedding matrix $\mathbf{H} \in \mathbb{R}^{N \times d}$ and the cluster centroid matrix $\mathbf{U} \in \mathbb{R}^{K \times d}$ by using the link formation probability module, respectively. In the first stage, *ClusterLP* takes \mathbf{U} as a fixed parameter to calculate the probability of building an edge between each node pair to obtain the predicted network adjacency matrix \mathbf{P} . The position of each node in the representation space is adjusted through backpropagation error by comparison $\mathbf{P}_{train} = \{\mathbf{P}_{ij} \mid e_{ij} \in \mathcal{E}_{train}\}$ with \mathbf{A}_{train} . Similarly, \mathbf{H} is used as a fixed parameter to update \mathbf{U} in the second phase. \mathbf{U} and \mathbf{H} adjusted after the above two stages can be used as the initial state of the next loop, and after multiple loop updates, *ClusterLP* will get stable \mathbf{U} and \mathbf{H} that fully capture the node relationships in the network. The effectiveness of link prediction can be evaluated by comparing the similarity of $\mathbf{P}_{test} = \{\mathbf{P}_{ij} \mid e_{ij} \in \mathcal{E}_{test}\}$ and \mathbf{A}_{test} .

1) *Initialize the cluster centroids:* Of course, we have noticed that many researches, such as softmax autoencoder, X-

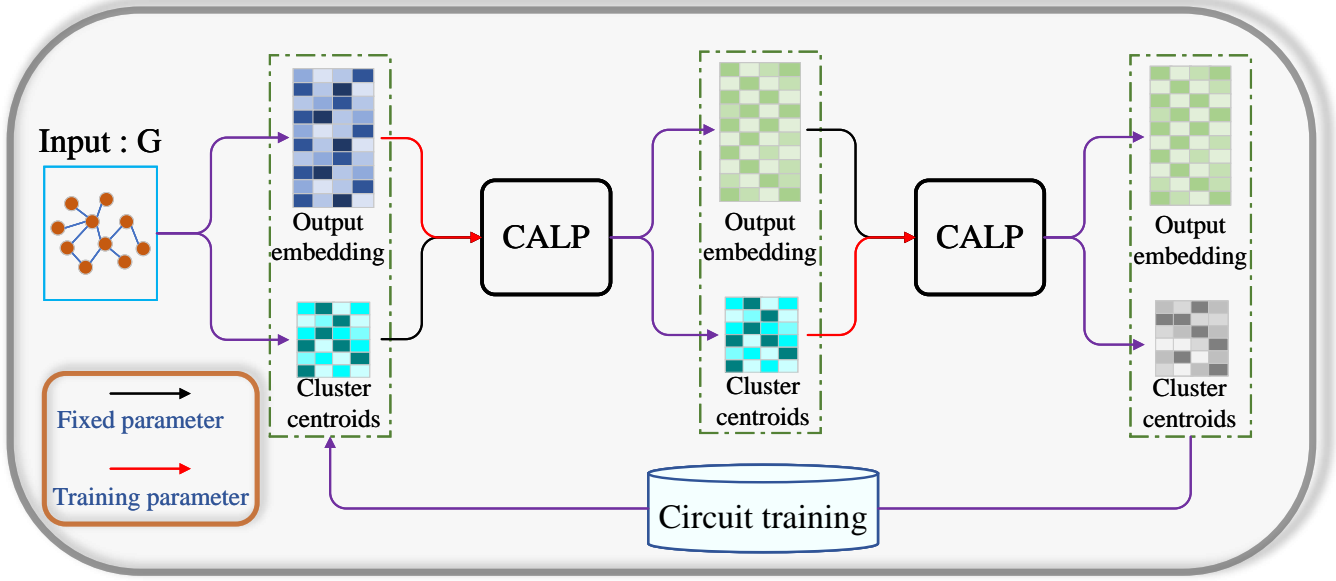


Fig. 3: Overall operation process of the proposed *ClusterLP* model.

means, G-means, etc., are committed to automatically selecting the optimal number of clusters in the clustering process. However, in our view, this does not fit perfectly with the ClusterLP framework, because the running process of ClusterLP is end-to-end at each stage, and a fixed \mathcal{K} will be necessary. How to introduce this automatic discrimination mechanism in ClusterLP will be our research direction in the next stage.

Given \mathcal{K} in the network, our goal is to select the best centroid for each cluster to reflect the location information of all nodes in the cluster to the greatest extent. For real-world networks, an ideal set of cluster centroids must fulfill two requirements:

- 1) The distance between the centroids should be large enough, meaning that the centroids are sufficiently dispersed. This requirement ensures that the trend difference from node to each cluster is sufficiently obvious.
- 2) The initial cluster centroids cannot be too far from the initial nodes representation. This requirement avoids the appearance of isolated clusters, where no nodes belong to these clusters.

The simplest initialization method is to randomly assign representation vectors to the centroids of these \mathcal{K} clusters, but it is difficult to guarantee the establishment of the above two conditions and cause unstable model performance. A method that is widely used in the field of complex network clustering and which we have performed well in practical applications is to perform \mathcal{K} -means clustering on the representation vectors of all nodes to obtain the initial cluster centroids. Given \mathcal{K} , this method is stable and can meet the above two requirements.

2) *Cluster-Aware Link formation Probability module (CALP)*: Probabilistic methods such as the Hierarchical Random Graph model [32] enlighten us that the cluster structure in the network can play an important role in estimating the probability of the existence of links, while the similarity-popularity methods such as HMSM [34] inspire us that it is not sufficient to only consider the similarity between nodes

when predicting the probability of links, and some global information such as the popularity of nodes can be additionally combined. We can't help but reasonably associate that if we replace $\phi(\kappa_i, \kappa_j)$ in Formula 1 with the cluster information of nodes, whether a new link prediction model that can combine the advantages of these two kind of models simultaneously will be generated?

In order to calculate the link formation probability between any two nodes in the network, our proposed *ClusterLP* will simultaneously preserve the *first-order proximity* and *cluster-level proximity* between nodes. Specifically, the *first-order proximity* U_{ij} between nodes v_i and v_j will be calculated by the similarity between the node representation vectors H_i and H_j , the cluster assignment t_i of node v_i will be calculated by H_i and cluster centroids U , the *cluster-level proximity* C_{ij} between v_i and v_j will be obtained by t_i and t_j , and finally the link formation probability P_{ij} between v_i and v_j will be calculated by D_{ij} and C_{ij} . The above procedure can be expressed as follows:

$$D_{ij} = \Omega(H_i, H_j) \quad (3)$$

$$T_{ik} = \Psi(H_i, U_k) \quad (4)$$

$$T_i = \Upsilon(T_{i1}, T_{i2}, \dots, T_{i\mathcal{K}}) \quad (5)$$

$$C_{ij} = \Phi(T_i, T_j) \quad (6)$$

$$P_{ij} = \Lambda(D_{ij}, C_{ij}) \quad (7)$$

In order to ensure that the operation of *ClusterLP* is end-to-end, the functions $\Omega(\cdot, \cdot)$, $\Psi(\cdot, \cdot)$, $\Upsilon(\cdot, \cdot)$, $\Phi(\cdot, \cdot)$ and $\Lambda(\cdot, \cdot)$ here must be differentiable. $\Omega(\cdot, \cdot)$, $\Psi(\cdot, \cdot)$ and $\Phi(\cdot, \cdot)$ are essentially calculating similarities between two vectors, and

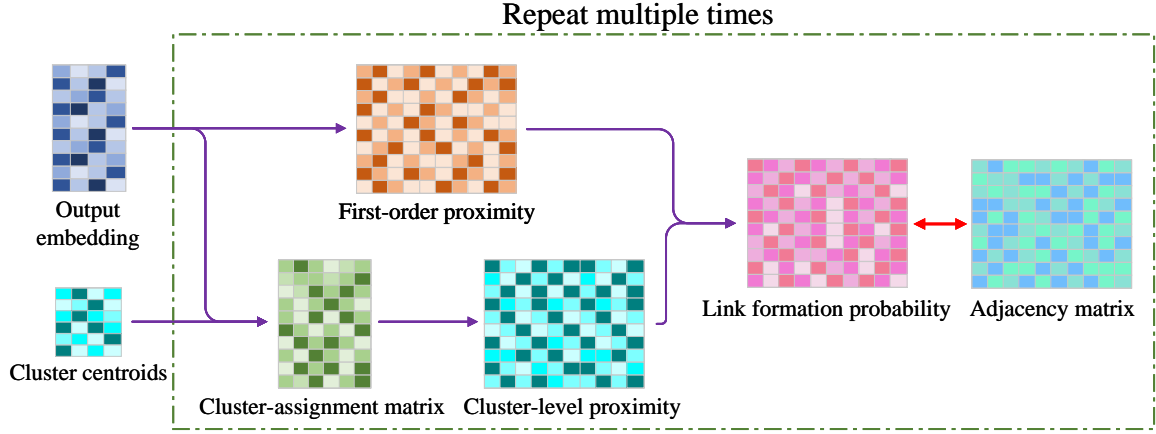


Fig. 4: Illustration of the proposed *CALP* module by simultaneously preserve the *first-order proximity* and *cluster-level proximity* between nodes.

it is important to note that $\Omega(\cdot, \cdot)$ and $\Psi(\cdot, \cdot)$ need to use the same similarity measurement method, and there can be no case such as the use of eumendic distances in $\Omega(\cdot, \cdot)$ and the use of dot products in $\Psi(\cdot, \cdot)$. This requirement is to maximize the correspondence of the relative positions of the nodes in the representation space to the true topology.

Algorithm 1 Link formation probability module.

Require: Output embedding matrix, $\mathbf{H} \in \mathbb{R}^{N \times d}$,
Cluster centroids, $\mathbf{U} \in \mathbb{R}^{K \times d}$;

- 1: **for** $i = 1$; $i < \text{epoch}$; $i++$ **do**
- 2: Calculating the first-order proximity \mathbf{D} of nodes using \mathbf{H} ;
- 3: Calculating the cluster-assignment matrix \mathbf{T} of nodes using \mathbf{H} and \mathbf{U} ;
- 4: Calculating the similarity between nodes at the cluster-level \mathbf{C} according to \mathbf{T} ;
- 5: Calculating the link forming probability between nodes \mathbf{P} using \mathbf{D} and \mathbf{C} ;
- 6: Calculating loss using \mathbf{P}_{train} to compare with \mathbf{A}_{train} and update \mathbf{H} or \mathbf{U} after error backpropagation;
- 7: **end for**
- 8: **return** Updated \mathbf{H} or \mathbf{U} ;

3) *Framework Learning Analysis*: With modeling the relationship between nodes in the network by using \mathbf{H} and \mathbf{U} , the final objective function of the proposed *ClusterLP* framework is formulated as follows:

$$\text{Loss} = \Gamma(\mathbf{P}_{train}, \mathbf{A}_{train}) \quad (8)$$

Because the set of links used in each training is invariant, the loss function described above is only related to \mathbf{H} and \mathbf{U} , which we can denote as $\mathcal{J}(\mathbf{H}, \mathbf{U})$. In each iteration, we update \mathbf{H} and \mathbf{U} iteratively, which hold the following inequality condition:

$$\mathcal{J}(\mathbf{H}^{(t+1)}, \mathbf{U}^{(t+1)}) \leq \mathcal{J}(\mathbf{H}^{(t+1)}, \mathbf{U}^{(t)}) \leq \mathcal{J}(\mathbf{H}^{(t)}, \mathbf{U}^{(t)}) \quad (9)$$

which proves the convergence of the proposed framework.

Based on the descriptions aforementioned, the main computational method of *ClusterLP* is to update the values of \mathbf{H} and \mathbf{U} by backpropagating the loss in each iteration, and the computational cost required for each update is $\mathcal{O}(N^2(d + K))$. Thus, the overall computational cost of *ClusterLP* is $\mathcal{O}(N^2(d + K))$, which is in the same order of magnitude as nonnegative matrix factorization and other node representation models incorporating the network community structure such as *NECS*[9].

D. Undirected graph link prediction model

In this section, we will instantiate the *ClusterLP* framework based on the characteristics of the undirected graph to obtain an efficient undirected graph link prediction model. In an undirected graph, the connection between nodes is undirected or bidirectional, for example, the friendship between two nodes (users) in a social network.

We will use the Euclidean distance between two vectors to calculate their *first-order proximity*, and define:

$$\mathbf{D}_{ij} = \Omega(\mathbf{H}_i, \mathbf{H}_j) = \|\mathbf{H}_i - \mathbf{H}_j\|^2 = \sqrt{\sum_{l=1}^d (\mathbf{H}_i^l - \mathbf{H}_j^l)^2} \quad (10)$$

$$\mathbf{T}_{ik} = \Psi(\mathbf{H}_i, \mathbf{U}_k) = \left(1 + \frac{\|\mathbf{U}_k - \mathbf{H}_i\|^2}{n}\right)^{-1} \quad (11)$$

To calculate a soft clustering assignment distribution of each node, we define the probability that node v_i belongs to cluster k as the tendency of vector \mathbf{H}_i to cluster centroid \mathbf{U}_k divided by the trend of \mathbf{H}_i to all the clustering centroids, which can be expressed as mathematical formula:

$$\begin{aligned} \mathbf{T}_i &= \Upsilon(\mathbf{T}_{i1}, \mathbf{T}_{i2}, \dots, \mathbf{T}_{iK}) \\ &= \left[\frac{\mathbf{T}_{i1}}{\sum_{l=1}^K \mathbf{T}_{il}}, \frac{\mathbf{T}_{i2}}{\sum_{l=1}^K \mathbf{T}_{il}}, \dots, \frac{\mathbf{T}_{iK}}{\sum_{l=1}^K \mathbf{T}_{il}} \right] \end{aligned} \quad (12)$$

Our definition of clustering assignmentment for nodes is an improvement on the Student's t-distribution used in *DAEGC*

[14], with only one more parameter n , so it does not break the advantages of being able to handle different scaled clusters and being computationally convenient. The hyperparameter n here is used to adjust the decay rate of cluster tendency, and the smaller n indicates that the cluster structure in the space is more obvious.

In order to capture the similarity between nodes v_i and v_j from a macroscopic perspective, we use cosine similarity to calculate the *cluster-level proximity* C_{ij} using the cluster assignment vectors \mathbf{T}_i and \mathbf{T}_j .

$$C_{ij} = \frac{\mathbf{T}_i \cdot \mathbf{T}_j}{\|\mathbf{T}_i\|^2 \cdot \|\mathbf{T}_j\|^2} = \frac{\sum_{k=1}^{\mathcal{K}} \mathbf{T}_{ik} \times \mathbf{T}_{jk}}{\sqrt{\sum_{k=1}^{\mathcal{K}} (\mathbf{T}_{ik})^2} \times \sqrt{\sum_{k=1}^{\mathcal{K}} (\mathbf{T}_{jk})^2}} \quad (13)$$

The definition shows that the closer C_{ij} is to 1, indicating that vectors \mathbf{T}_i and \mathbf{T}_j are more similar, otherwise the similarity is smaller. We also use the max abs normalization for \mathbf{D} to limit the values of each of its elements to between 0 and 1, and obviously, a small value of \mathbf{D}_{ij} favors the formation of link between v_i and v_j .

$$\mathbf{D} = \frac{\mathbf{D}}{\max(\mathbf{D})} \quad (14)$$

According to the previous analysis, the probability of forming a link between two nodes is proportional to their *cluster-level proximity*, and inversely proportional to the *first-order proximity* between them, which can be expressed in a formula.

$$\mathbf{P} \propto \frac{\mathbf{C}}{\mathbf{D}} \quad (15)$$

There are many mathematical tools for modeling such relationships, including the widely used sigmoid function, and we have chosen a simple power function here due to its computationally simple and excellent convergence effect:

$$\mathbf{P}_{ij} = \Lambda(\mathbf{D}_{ij}, \mathbf{C}_{ij}) = \exp\left(-\beta \frac{\mathbf{D}_{ij}}{\mathbf{C}_{ij}}\right) \quad (16)$$

The larger the β value, the greater the influence of *first-order proximity* between nodes on link formation, indicating that the cluster structure of the network is not obvious. Setting an excessively large β causes the node representation vectors of the final output to gather together with little difference, resulting in an increased probability of forming links between nodes, and a significant increase in the density of links in the reconstructed network compared to real networks. The smaller the β value, the greater the impact of *cluster-level proximity* on link formation, and the more obvious the cluster structure of the network. Setting a small β will result in a very small probability of nodes in different clusters forming links, which will result in multiple isolated clusters in the reconstructed network, that is, the network is not connected.

In many experiments, we found that 4 and 5 are the upper and lower thresholds of β , respectively. We conducted network reconstruction experiments using multiple networks, and found that the network reconstructed generally has isolated clusters when $\beta = 4$, while the reconstructed network is significantly

denser than the real network when $\beta = 5$, so we recommend the value range of β as [4, 5].

We choose the *Mean Square Error (MSE)* as loss function to calculate error and *SGD* with learning rate η and momentum δ as optimizer to adjust the parameters:

$$\mathcal{L} = \frac{\|\mathbf{P}_{train} - \mathbf{A}_{train}\|^2}{|\mathbf{A}_{train}|} \quad (17)$$

Connection to NECS[9]. NECS also preserves the high-order proximity and incorporates the community structure in vertex representation learning, which attempts to optimize the following objective function:

$$\begin{aligned} \min_{\mathbf{U}, \mathbf{V}, \mathbf{W}, \mathbf{H}} & \|\mathbf{P} - \mathbf{V}\mathbf{U}^T\|_F^2 + \alpha \|\mathbf{S} - \mathbf{H}\mathbf{H}^T\|_F^2 \\ & + \beta \|\mathbf{H} - \mathbf{U}\mathbf{W}^T\|_F^2 + \lambda \|\mathbf{H}^T\mathbf{H} - \mathbf{I}\|_F^2 \\ s.t. & \mathbf{V} \geq 0, \mathbf{U} \geq 0, \mathbf{W} \geq 0, \mathbf{H} \geq 0, \mathbf{H}\mathbf{1} = \mathbf{1} \end{aligned} \quad (18)$$

where \mathbf{P} is a high-order proximity of adjacency matrix \mathbf{A} ; the positive semi-definite matrix $\mathbf{U}, \mathbf{V} \in \mathbb{R}^{N \times d}$ are the low-dimensional representations of vertices; \mathbf{S} is the similarity between two arbitrary vertices, defined as $\mathbf{S}_{ij} = \mathbf{A}_{i*} \mathbf{A}_{*j} / \|\mathbf{A}_{i*}\| \|\mathbf{A}_{*j}\|$; $\mathbf{H} = [\mathbf{H}_{ir}] \in \mathbb{R}^{N \times k}$, where $[\mathbf{H}_{ir}]$ is viewed as the probability of v_i belonging to community c_r ; $\mathbf{W} \in \mathbb{R}^{k \times d}$, where r -th row of \mathbf{W} (i.e., \mathbf{W}_{r*}) is the representation of community c_r .

Clearly, the \mathbf{U} , \mathbf{W} and \mathbf{H} used in NECS corresponds to \mathbf{H} , \mathbf{U} and \mathbf{T} of *ClusterLP*, respectively. Compared with NECS, our proposed *ClusterLP* has at least the following three advantages:

- Fewer parameters. As can be seen from our description above, for *ClusterLP*, the optimization targets of the last two in Formula.18 do not exist, and only one representation vector is required for each node, thus the total number of parameters can be reduced from $\mathcal{N} \times (2d + \mathcal{K}) + \mathcal{K} \times d$ of NECS to our $(N + \mathcal{K}) \times d$;
- Faster operational efficiency. The objective function of NECS is not jointly convex, so it cannot optimize all the variables \mathbf{U} , \mathbf{V} , \mathbf{W} and \mathbf{H} simultaneously, only to use an alternating optimization algorithm to learn one variable while fixing others. While Our *ClusterLP* only needs to update \mathbf{H} and \mathbf{U} alternately.
- Stronger structural expression ability. NECS believed that if vertices are more similar to each other, they are more likely to belong to the same community, and thus defined the matrix \mathbf{S} . However, such a definition is rough because the similarity between any pair of nodes without a common neighbor node is calculated as 0, even if the *first-order proximity* between them is 1. Comparatively, the *cluster-level proximity* we define can more accurately and comprehensively capture the higher-order similarity between nodes.

E. Directed graph link prediction model

Links in a directed network has the notion of direction, that is, the relationships between nodes are not equal. For

example, in the citation networks, a node v_i (a paper/book) will reference another node v_j , but because of the irreversibility of time, v_j will most likely not reference v_i . Of course, some directed networks allow two nodes to refer to each other, such as a network composed of hyperlinks of websites.

The application of *ClusterLP* framework to a directed graph can be simply understood as nodes tend to form links to nodes that are similar to their own representation vectors and have an important position (high popularity) in their own clusters. Whether in a directed or undirected graph, the probability of forming a link between nodes representing more similar vectors is always greater. For example, in a citation network, an article always tends to cite another article with similar research content; in social networks, a user is often willing to make friends with another user with similar interests.

Our main innovation compared to the similarity-popularity methods and *Gravity-GAE* is the introduction of cluster-aware in nodes popularity. In the previous works, the popularity of node v_i was the same for the rest of the nodes in the network, which is inconsistent with the real network. Taking a realistic example, although article A (such as *LeNet-5* [37]) has a very authoritative position in one research field (*CV*), but in the view of article B in another field (*GNN*), the reference value of A is very small, so B will most likely not cite A . This change can greatly reduce redundant links (links that do not exist in \mathbf{A} but exist in the prediction network), and thus improve the prediction ability of our model.

We still use the Euclidean distance to calculate the *first-order proximity* between two nodes in a directed graph:

$$\mathbf{D}_{ij} = \Omega(\mathbf{H}_i, \mathbf{H}_j) = \|\mathbf{H}_i - \mathbf{H}_j\|^2 = \sqrt{\sum_{l=1}^d (\mathbf{H}_i^l - \mathbf{H}_j^l)^2} \quad (19)$$

$$\mathbf{D} = \frac{\mathbf{D}}{\max(\mathbf{D})} \quad (20)$$

To reflect the directivity of the link, we made adjustments when calculating the *cluster-level proximity* between nodes v_i and v_j . Specifically, 1) the similarity calculation for cluster assignment vectors \mathbf{T}_i and \mathbf{T}_j is adjusted from the cosine similarity used in the undirected graph to the directional version, so that $\mathbf{C}_{ij} \neq \mathbf{C}_{ji}$; 2) The normalization used in the undirected graph is eliminated when calculating \mathbf{T}_i and \mathbf{T}_j , because we need to use the tendency of nodes to each cluster; 3) The tendency \mathbf{T}_{ik} of vector \mathbf{H}_i to cluster centroid \mathbf{U}_k changes from $(0, 1]$ in the undirected graph to $(1, n + 1]$, which is necessary and effective because it avoids the following exception.

$$\mathbf{T}_{ik} = \Psi(\mathbf{H}_i, \mathbf{U}_k) = \frac{n}{1 + \|\mathbf{U}_k - \mathbf{H}_i\|^2} + 1 \quad (21)$$

$$\mathbf{T}_i = \Upsilon(\mathbf{T}_{i1}, \mathbf{T}_{i2}, \dots, \mathbf{T}_{iK}) = [\mathbf{T}_{i1}, \mathbf{T}_{i2}, \dots, \mathbf{T}_{iK}] \quad (22)$$

$$\mathbf{C}_{ij} = \frac{\mathbf{T}_i \cdot \mathbf{T}_j}{\|\mathbf{T}_i\|^2 \cdot \|\mathbf{T}_j\|^2} = \frac{\sum_{k=1}^K \mathbf{T}_{ik} \times \mathbf{T}_{jk}}{\sum_{k=1}^K (\mathbf{T}_{ik})^2} \quad (23)$$

Exception (*Extreme situation of cluster tendency distribution*) This exception occurs when we use Formula.11 to calculate the cluster tendency of nodes, where a node v_i has a strong tendency to a certain number of clusters will resulting in many nodes have a great *cluster-level proximity* with v_i calculated by Formula.23, which causes the generation of a large number of redundant links and damages the prediction performance of our model. Here's an example: suppose $K = 3$, the cluster assignment vector calculated by nodes v_i and v_j is $\mathbf{T}_i = [0.05, 0.05, 0.05]$ and $\mathbf{T}_j = [0.9, 0.9, 0.9]$ respectively, in this case, the probability of a directed link from v_i to v_j calculated is $\mathbf{C}_{ij} = 45$. Obviously, node v_i has a strong attraction to the edge nodes, and theoretically, when using Formula.11, the value range of any element \mathbf{C}_{ij} in \mathbf{C} is $(0, \infty)$.

In order to limit the range of values of elements in \mathbf{C} , we propose Formula.21 to replace Formula.11, at which point the value range of \mathbf{C}_{ij} can be narrowed to $(0, n + 1)$, and a suitable n can be selected to perfectly avoid the occurrence of the above abnormal situation.

As with the undirected graph, the formation probability \mathbf{P}_{ij} of a directed link from v_i to v_j is proportional to \mathbf{C}_{ij} and inversely proportional to \mathbf{D}_{ij} . We still use power function to model this relationship, and choose *MSE* and *SGD* to optimize \mathbf{H} and \mathbf{U} :

$$\mathbf{P}_{ij} = \Lambda(\mathbf{D}_{ij}, \mathbf{C}_{ij}) = \exp\left(-\beta \frac{\mathbf{D}_{ij}}{\mathbf{C}_{ij}}\right) \quad (24)$$

$$\mathcal{L} = \frac{\|\mathbf{P}_{train} - \mathbf{A}_{train}\|^2}{|\mathbf{A}_{train}|} \quad (25)$$

IV. EXPERIMENTAL ANALYSIS

To validate the effectiveness of our *CluetrLP* framework, a series of experiments is conducted on link prediction tasks using multiple types of real-world datasets. Graphs are unweighted and featureless, and details of them are summarised in Table II.

There are totally four hyperparameters in *ClusterLP*: the number of clusters K , the node representing vector dimension d , the tightness of clusters in the representation space n and β , which controls the relative importance of *first-order proximity* and *cluster-level proximity*. Within a certain range, setting a larger K can enable *ClusterLP* to master more global information about the network. However, when the value of K becomes too large, it will not only bring about an expansion of time and space complexity, but also make the model pay too much attention to micro information, thus losing the grasp of macro information. Similarly, a high-dimensional representation vector can describe the characteristics of each node more comprehensively, but this can lead to problems of inadequate model training and explosive complexity. Our multiple experiments have shown that a general and ideal option is setting K to 12 and d to 8 for small networks, setting K to 24 and d to 12 for medium-size networks. The values of those parameters we set in the subsequent experiments are also summarized in Table II.

TABLE II: Statistics of experimental datasets and parameters setting.

Type	Datasets	Statistics of networks			Parameters setting					
		Nodes	Edges	Avg. degree	\mathcal{K}	d	n	β	η	δ
Undirected ¹	Citeseer	3327	4552	1.37	24	12	5	4.5	0.4	0.9
	Cora	2708	5278	1.95			4.5	4.5		
	Wiki	2405	11596	4.82			5	4.5		
	C.ele	297	2148	7.23			5	4.2		
	Wisconsin	251	450	1.79			5	4.8		
	Texas	183	279	1.52			4.8	4.2		
	Email	986	16064	16.29	12	8	5	4.5	0.1	
	Polbooks	105	441	4.20			5	4.5		
	Karate	34	78	2.29			1	5		
Directed ²	Citeseer	3327	4732	-	48	12	25	5.0	0.01	0.9
	Cora	2708	5429	-				4.8		
	Wisconsin	251	499	-				4.8		
	Cornell	183	295	-				5		

A. Undirected graph link prediction

In this section, we first introduce the baseline methods used for comparison, then perform a network reconstruction experiment on a small network **Karate** to verify the strong ability of *ClusterLP* to capture the link relationship between nodes, and finally we will perform link prediction experiments in incomplete networks to prove the strong generalization ability of *ClusterLP*.

1) *Baseline Methods*: Not only do we compare *ClusterLP* with the classic models *LINE*, *Node2vec* and *GIC* described in Chapter 2, but we also add several more state-of-the-art models to fully demonstrate the effectiveness of our model:

- Our own *JPA*, combined three heuristic link prediction methods *JC*, *Preferential Attachment*[31] and *AA* to obtain the topology information between nodes, and then *Random Forest* is used to predict the link formation probability;
- *VGAE*[19] is a variational graph autoencoder approach for graph embedding with both topological and content information;
- *ARVGA*[18] adds adversarial constraints to *VGAE*, enforcing the latent representations to match a prior distribution for robust node embeddings;
- *AGE*[17], while like *ClusterLP* requires computing the similarity between nodes, it only uses the node embeddings obtained by first smoothly filtering the node features through t -layer Laplace followed by linear transformation without exploiting the cluster structure;
- *Linear Modularity-Aware VGAE (LMA)*[8] introduces and theoretically study a community-preserving message passing scheme, doping *VGAE* encoder by considering both the initial graph structure and modularity-based prior communities when computing embedding spaces;
- *NAFS*[2] first extracts the features of each node with its neighbors of different hops by feature smoothing, then adaptively combines the smoothed features, and finally the constructed node representation can further be enhanced by the ensemble of smoothed features extracted via different smoothing strategies;
- *MAD*[10] introduces an additional component called *Memory* to memorize all the training data, then learns

the differences of labels as well as the associations of features in the combination of a differential equation and some sampling methods, and finally predicts unknown labels by inferencing from the memorized facts plus the learnt differences and associations in a geometrically meaningful manner.

Note that since we are committed to studying how to use only the topology of the network to model the link relationship between nodes, for comparison methods such as *VGAE* that need to use node attributes \mathcal{F} , we uniformly use the identity matrix $\mathcal{I} \in \mathbb{R}^{|\mathcal{V}| \times |\mathcal{V}|}$ to replace \mathcal{F} .

2) *Network reconstruction*: In order to fully verify the excellent expression ability of *ClusterLP*, we will take the well-studied **karate** network as an example, take the complete network as input, train repeatedly to obtain the representation vector of each node and cluster centroid, and finally calculate the probability of forming a link between each pair of nodes to obtain the prediction network. Table III reports the effect of the reconstructed network using different link prediction models on four evaluation indicators, Fig.5 is a schematic diagram of the reconstruction results of Karate network using *ClusterLP* and *VAGE* respectively.

Obviously, the results show that *ClusterLP* has achieved an overwhelming advantage in this task compared to the baseline models. In order to explore the reasons why *ClusterLP* works so effectively, a careful observation of these four indicators shows that *ClusterLP* has little advantage on the *ACC* indicator, and several baseline models can basically be on par with it; however, on the *AP* indicator, *ClusterLP* shows superior performance, leaving the rest of models far behind, which shows that: 1) Like other excellent models, the nodes representation vector obtained by *ClusterLP* can accurately describe the existence of real links in the network; 2) Compared with other models, *ClusterLP* can more accurately determine links that do not exist in the network, which can be proved by the fact that the number of links in the network reconstructed by *ClusterLP* is very close to the actual number of links, while in networks reconstructed by other models, the number of links is much greater than the actual value.

¹Mainly borrowed from *NECS*[9]

²Mainly borrowed from *DiGAE*[6]

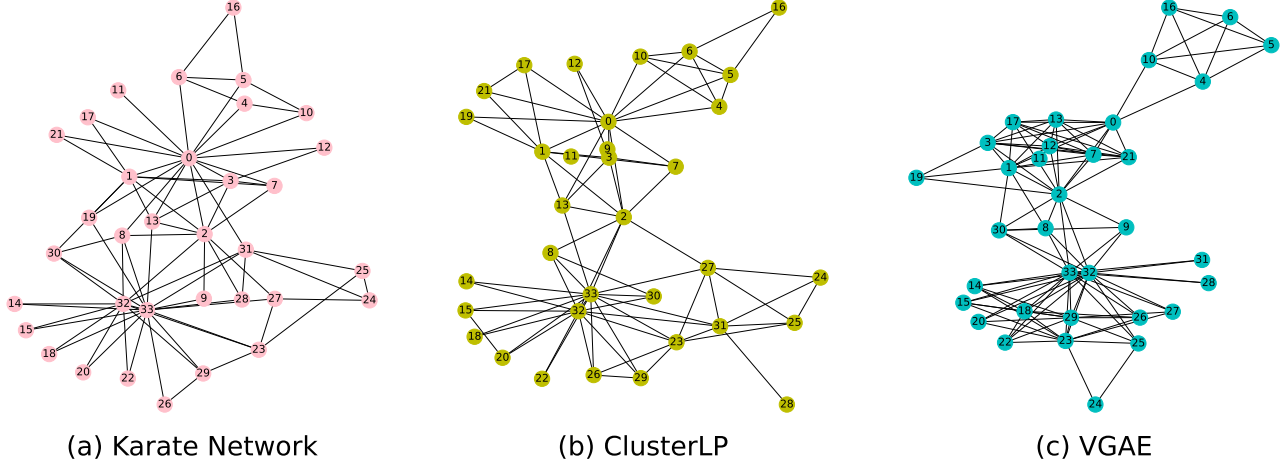


Fig. 5: Embedding-based link prediction methods take a complete adjacency matrix as input and produces a representation vector for each node in the network in \mathbb{D}^d as output. (a) shows the original **Karate** network, which has 34 nodes and 78 undirected edges; (b) and (c) are the result of reconstructed **Karate** network using the output of *ClusterLP* and *VGAE*, respectively. More reconstructed networks can be found in the Appendix.

TABLE III: Comparison of *ClusterLP* with other link prediction models in the reconstruction of **karate** task.

Models	links	Accuracy	Precision	Recall	F1 Score
<i>LINE</i>	118	90.16	74.48	82.74	78.39
<i>Node2vec</i>	134	85.66	73.42	80.22	76.67
<i>NECS</i>	75	82.53	62.12	61.33	61.70
<i>VGAE</i>	114	88.93	76.56	86.03	80.01
<i>ARVGA</i>	71	93.25	86.46	83.66	84.98
<i>AGE</i>	82	93.77	86.19	87.74	86.94
<i>GIC</i>	85	87.02	72.43	74.11	73.22
<i>LMA</i>	82	<u>94.12</u>	<u>86.90</u>	88.48	<u>87.67</u>
<i>NAFS</i>	85	93.94	86.23	<u>88.93</u>	87.50
<i>ClusterLP</i>	79	96.71	92.77	93.23	93.00

3) *Results for Undirected Link Prediction*: To assess the performance of our proposed method, we randomly select 90% of existing links and 4 times the number of non-existed links as training samples, while the remaining existing links and the same number of non-existed links are taken as test samples. For the experimental results, we report the mean area under the ROC curve (**AUC**) and the average precision (**AP**) scores over ten trials with different random seeds and train/test splits.

Comparison on prediction quality in terms of the two evaluation metrics is shown in Table IV, from which, the following conclusions can be observed:

- The proposed *ClusterLP*, considering both *cluster-level proximity* and *first-order proximity*, performs better on all networks than *GIC* suggesting that introducing cluster-level information content into the generation of node representation vectors, rather than just as an auxiliary information to adjust the obtained representation vectors, may be able to capture this higher-order information of networks more effectively. Moreover, *ClusterLP* even

show good performance compared to the heuristic method *JPA* in all datasets as it can capture structural information that *JPA* utilize.

- We can observe that *ClusterLP* consistently achieves state-of-the-art performance on the first five datasets. Especially, *ClusterLP* show significant improvements on **Texas** and **Wisconsin**, where the improvements of *ClusterLP* over the best baseline are 6.17% and 4.97% on **AUC**, 1.79% and 3.21% on **AP**, respectively.
- Texas** is a very special network. First, We note that conventional feature-based GNNs such as *VGAE* show poor performance with a huge gap than that of node similarity-based methods on **Texas**. This implies that feature-based GNNs have a difficulty in directly utilizing structural information e.g., degree and overlapped neighbors, for link prediction. According to this implication, *ClusterLP* and *LINE* are able to learn structural information, thus these methods accomplish better performance than conventional GNNs do; Furthermore, many models show huge differences in **AP** and **AUC**, typical examples are *VGAE*, *AGE*, *ARVGA* and *NAFS*, whose **AP** are more than 10% larger than their **AUC**. While models which can use network topology information like *JPA*, generally have a larger **AUC**.
- In the last three larger networks, the performance of *ClusterLP* is worse than that of *AGE* and *NAFS*, but better than other baseline methods. We believe this is because reconstruction-based methods (e.g., *ClusterLP* and *GIC*) overestimate the existing node links (they reconstruct the adjacency matrix), which favors small datasets like **Polbooks**. In addition, the type of network is also an important factor, as the last three networks are all citation networks and are structurally different from the first five.

4) *Parameter Analysis*: In this subsection, we choose **C. ele** network and employ the GridSearchCV to learn the default

TABLE IV: Undirected link prediction performances (%) of our *ClusterLP* and baselines on eight datasets. Each number is the average performance for 10 random initialization of the experiments. **Bold** indicates the best performance and underline indicates the second best performance.

Metrics	Models	Polbooks	Texas	Email	Wisconsin	C.ele	Wiki	Cora	Citeseer
AP	<i>JPA</i>	73.71 \pm 4.58	59.70 \pm 4.44	81.74 \pm 0.62	65.80 \pm 3.61	73.70 \pm 2.03	88.30 \pm 0.71	73.93 \pm 0.89	66.77 \pm 1.06
	<i>LINE</i>	69.70 \pm 5.86	67.45 \pm 4.72	80.86 \pm 0.56	71.53 \pm 4.04	75.80 \pm 1.04	88.56 \pm 0.67	80.18 \pm 0.65	81.07 \pm 1.08
	<i>Node2vec</i>	78.63 \pm 3.23	69.83 \pm 5.68	78.63 \pm 0.62	72.36 \pm 4.35	71.61 \pm 1.86	87.14 \pm 0.56	89.01 \pm 0.40	82.05 \pm 0.57
	<i>VGAE</i>	<u>88.74 \pm 5.88</u>	55.69 \pm 6.32	90.34 \pm 0.55	72.52 \pm 4.25	78.32 \pm 3.49	93.07 \pm 0.54	89.38 \pm 0.66	84.39 \pm 1.34
	<i>ARVGA</i>	<u>82.81 \pm 2.67</u>	<u>74.36 \pm 3.98</u>	88.24 \pm 0.61	<u>83.52 \pm 2.73</u>	81.92 \pm 1.91	93.05 \pm 0.46	89.51 \pm 0.72	84.39 \pm 0.89
	<i>AGE</i>	85.93 \pm 3.22	73.44 \pm 6.67	86.31 \pm 0.59	81.93 \pm 3.20	81.70 \pm 2.05	<u>94.23 \pm 0.34</u>	92.43 \pm 0.80	89.85 \pm 1.58
	<i>GIC</i>	87.20 \pm 3.29	44.38 \pm 6.01	84.16 \pm 0.71	58.55 \pm 7.15	74.31 \pm 3.28	88.12 \pm 0.73	83.73 \pm 0.85	87.09 \pm 0.64
	<i>LMA</i>	87.33 \pm 3.66	62.39 \pm 5.76	<u>91.42 \pm 0.36</u>	74.37 \pm 3.92	83.39 \pm 1.87	93.44 \pm 0.37	89.36 \pm 0.88	83.47 \pm 1.01
	<i>MAD</i>	86.91 \pm 2.11	65.77 \pm 3.69	91.08 \pm 0.38	72.80 \pm 3.15	<u>87.04 \pm 1.12</u>	92.58 \pm 0.22	84.81 \pm 0.52	75.44 \pm 0.30
	<i>NAFS</i>	87.80 \pm 3.86	63.54 \pm 8.26	90.18 \pm 0.55	78.71 \pm 2.57	81.20 \pm 1.77	95.16 \pm 0.39	<u>89.88 \pm 0.87</u>	81.96 \pm 0.67
	<i>ClusterLP</i>	92.71 \pm 1.72	75.69 \pm 2.93	91.51 \pm 0.17	86.20 \pm 2.21	87.81 \pm 1.11	93.62 \pm 0.83	88.85 \pm 1.25	<u>87.30 \pm 1.07</u>
AUC	<i>JPA</i>	79.56 \pm 4.07	63.04 \pm 5.42	86.86 \pm 0.47	70.78 \pm 3.79	80.04 \pm 1.84	91.03 \pm 0.50	78.87 \pm 0.77	72.18 \pm 1.02
	<i>LINE</i>	75.33 \pm 5.44	<u>72.50 \pm 4.67</u>	86.00 \pm 0.42	76.33 \pm 3.65	81.78 \pm 0.98	90.45 \pm 0.55	84.75 \pm 0.55	<u>85.91 \pm 0.80</u>
	<i>Node2vec</i>	83.22 \pm 2.13	71.43 \pm 4.72	82.58 \pm 0.66	73.78 \pm 4.25	76.44 \pm 1.46	88.25 \pm 0.57	86.02 \pm 0.68	74.62 \pm 1.00
	<i>VGAE</i>	<u>90.95 \pm 3.30</u>	39.42 \pm 8.45	89.61 \pm 0.54	62.32 \pm 5.88	81.80 \pm 2.18	90.82 \pm 0.63	86.20 \pm 0.81	79.39 \pm 1.60
	<i>ARVGA</i>	90.14 \pm 2.57	64.75 \pm 3.79	88.27 \pm 0.57	76.37 \pm 2.97	83.32 \pm 1.39	90.58 \pm 0.57	85.70 \pm 0.79	79.16 \pm 1.02
	<i>AGE</i>	86.75 \pm 2.28	65.86 \pm 5.88	85.61 \pm 0.64	<u>78.31 \pm 4.72</u>	83.30 \pm 1.44	<u>93.54 \pm 0.43</u>	91.31 \pm 0.98	87.39 \pm 1.94
	<i>GIC</i>	85.82 \pm 3.25	54.53 \pm 5.09	83.98 \pm 0.97	66.49 \pm 6.25	76.11 \pm 2.44	83.91 \pm 1.11	79.79 \pm 1.07	83.44 \pm 0.86
	<i>LMA</i>	88.28 \pm 2.45	48.59 \pm 5.18	90.65 \pm 0.35	65.79 \pm 3.80	84.70 \pm 1.63	91.11 \pm 0.58	86.47 \pm 1.05	78.99 \pm 1.36
	<i>MAD</i>	87.45 \pm 1.82	68.82 \pm 3.41	91.25 \pm 0.16	71.62 \pm 3.09	<u>88.78 \pm 0.51</u>	90.99 \pm 0.32	80.40 \pm 0.53	68.34 \pm 0.60
	<i>NAFS</i>	88.21 \pm 3.54	53.67 \pm 9.31	<u>91.73 \pm 0.39</u>	70.68 \pm 3.90	83.05 \pm 1.52	93.97 \pm 0.49	84.68 \pm 1.48	77.07 \pm 0.69
	<i>ClusterLP</i>	91.23 \pm 2.86	75.84 \pm 2.79	92.21 \pm 0.19	82.20 \pm 2.38	88.93 \pm 0.64	93.18 \pm 0.69	<u>87.59 \pm 0.93</u>	84.73 \pm 0.81

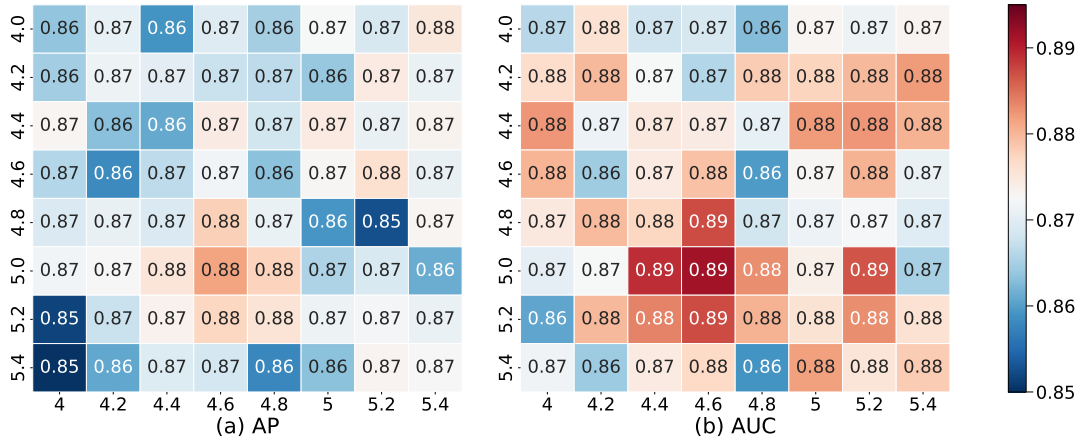


Fig. 6: Parameter analysis of β and n on **C.ele** network. In each subfigure, the horizontal x-axis indicates the distribution of β ; and the vertical y-axis reflects the distribution of n .

parameter settings of β and n in *ClusterLP*. To be specific, we specify β and n to be $\{4.0, 4.2, 4.4, 4.6, 4.8, 5.0, 5.2, 5.4\}$, respectively. Fig.6 reports the changes of two evaluation metrics w.r.t. different parameter combinations.

The role of parameters β and n has been analyzed in the previous content, and we can observe two phenomena from Fig.6: (a) the prediction effect of *ClusterLP* is not sensitive to small changes in individual β and n , which is manifested in the color change of the adjacent two boxes in the figure is not drastic; (b) the best performing parameter settings for *ClusterLP* are $\beta = 4.6$, $n = 5.0$, and the sub optimal ones are $\beta = 5.2$, $n = 4.4$, which is reflected in the box color around

these two parameter pairs in Fig.6 is darker red. The above two points are also reflected in the parameter settings we have listed in detail in Table II.

B. Directed graph link prediction

In this section, we empirically evaluate and discuss the performance of *ClusterLP* on four real-world datasets and two variants of the directed link prediction problem.

1) *Two Directed Link Prediction Tasks*: We consider the following learning task for our experiments.

Biased Negative Samples (B.N.S.) Link Prediction[3]. For this task, we train models on incomplete versions of

graphs where 10% of edges were removed for the test set. However, removed edges are all unidirectional, i.e., (i, j) exists but not (j, i) . The reverse node pairs are included in the test set in this setting. They constitute negative samples. In other words, all node pairs from test sets are included in both directions. We evaluate the performance of our models on a binary classification task consisting in identifying actual edges from fake ones, and therefore evaluate the ability of our models to correctly reconstruct $\mathbf{A}_{ij} = 1$ and $\mathbf{A}_{ji} = 0$ simultaneously. This task is very challenging as the ability to reconstruct asymmetric relations is now crucial and models ignoring directionality and only learning the symmetric graph proximity, such as standard *graph AE* and *VAE*, will fail in such a setting (they would always return $p_{ij} = p_{ji}$).

Bidirectionality Prediction[5]. This second evaluation task also strongly relies on directionality learning. We evaluate the ability of our models to identify bidirectional edges, i.e., reciprocal connections, from unidirectional edges. We create an incomplete training graph by randomly removing one of the two directions of all bidirectional edges. Therefore, the training graph only includes unidirectional connections. Then, we again consider a binary classification problem. We aim to retrieve bidirectional edges in a test set composed of their removed direction and of the same number of reverse directions from true unidirectional edges (that are, therefore, fake edges). In other words, for each pair of nodes v_i, v_j from the test set, we observe a connection from v_j to v_i in the incomplete training graph, but only half of them are reciprocal.

2) *Baseline Methods:* Besides comparing the performance of our methods to the alternative graph embedding method *Gravity-GAE* mentioned before, we have also collected and compared some models that apply to directed link prediction: *HOPE*[4] aims to preserving asymmetric transitivity by approximating high-order proximity which are based on asymmetric transitivity; *APP*[3] is an asymmetric proximity preserving graph embedding method via random walk with restart, which captures both asymmetric and high-order similarities between node pairs; *Source/Target Graph VAE*[5], extending the source/target vectors paradigm to *VGAE*, and trained with similar settings w.r.t. standard gravity models; *DiGAE*[6] learns pairs of interpretable latent representations for the nodes of directed graphs, and uses parameterized graph convolutional network (GCN) layers for its encoder and an asymmetric inner product decoder; *MVGAE*[22] first uses an efficient motif adjacency matrix learning algorithm, which can be used to extract high-order structures in directed networks, and construct multiple motif adjacency matrices, then extends *VGAE* to solve the link prediction problem in directed networks.

3) *Results for Directed Link Prediction:* Table V reports the mean AUC and AP scores, along with standard errors over 10 runs, for each dataset and the two tasks. Overall, our *ClusterLP* achieve competitive results.

- On both tasks and all four datasets, our proposed *ClusterLP* is superior to *Gravity GAE*, which shows that using the representation vectors of nodes to calculate their influence, that is, adding a cluster constraint to the influence of each node, can not only reduce the number of

parameters to be trained from $N \times (d + 1)$ to $(N + K) \times d$, but also greatly reduce the number of redundant links.

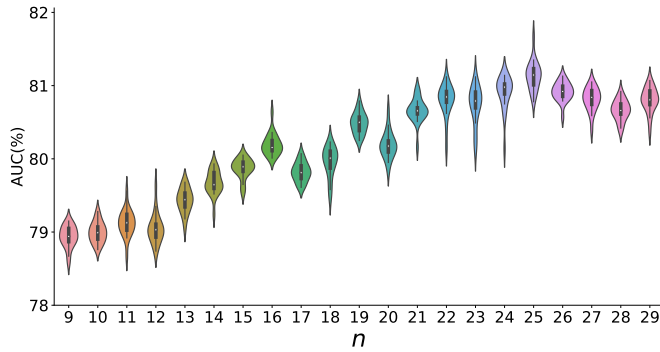
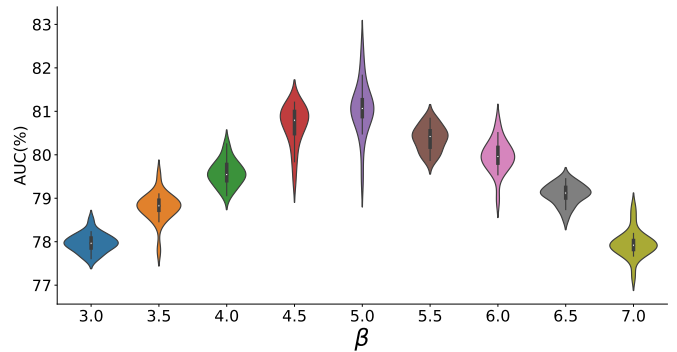
- While models ignoring the directionality for prediction, e.g., standard *VGAE*, totally fail (50.00% **AUC** and **AP** on all graphs, corresponding to the random classifier level), which was expected since test sets include both directions of each node pair.
- Experiments on task 2, i.e., on bidirectionality prediction, confirm the superiority of our approach when dealing with tasks where directionality learning is crucial. Indeed, on this last task, *Gravity VAE* also outperform the alternative approaches, indicating that the introduction of influence on nodes can indeed effectively determine the directionality of links.
- An interesting phenomenon we found is that, on task 1, *ClusterLP* and *Gravity GAE* perform well on **Cora** and **Citeseer**, but perform worst among all models (except for *VGAE*) with very large variances on the last two small datasets. In our experiments, we found that there were very few links that met the requirements of this task in **Cornell** and **Wisconsin**, with only 233 and 361 positive links in the training set, respectively. We believe that inadequate training is the main reason for the poor and unstable performance of these two influence-inspired models, because they have more parameters to train. There are two main bases for our judgment: (a) According to the previous description of the two tasks, it can be found that task two is more challenging, which can be proved in several places in Table V (e.g., the performance of *ClusterLP* and *Gravity GAE* on the **Cora** and **Citeseer** datasets, and the performance of baseline models such as *DiGAE*, *MVGAE* and *LINE* on four datasets). Therefore, under normal circumstances, for **Cornell** and **Wisconsin**, *ClusterLP* and *Gravity GAE* should perform better on Task 1 than they do on Task 2, but the expected experimental results do not appear in Table V; (b) The positive links in the training set of **Cornell** and **Wisconsin** in Task 2 were 277 and 450, respectively, a significant increase from Task 1. At the same time, compared with task 1, the two models not only increased the mean AUC and AP significantly on task 2, but also narrowed their variances.

4) *Discussion:* To complete our experimental analysis, we propose a discussion on the nature of n , on the role of β to balance node proximity and influence, and on some extensions of our approach. In Fig.7 and Fig.8, we use the **Citeseer** dataset as an example to show the impact of n and β on the AUC score of *ClusterLP*, respectively (Violin plots of the results of 10 runs with different parameter settings is reported.).

- **Deeper insights on n .** The expectation of our decoding scheme is that nodes with less influence tend to be connected to nodes with greater influence from their embedded neighborhood, where we define the influence of a node as the set of distances from the node to the centroid of various clusters. n is the most critical parameter when calculating the influence of a node, because it controls how quickly the influence in a single cluster

TABLE V: Directed link prediction on the Cora, Citeseer, Cornell and Wisconsin graphs.

Metrics	Methods	B.N.S. Link Prediction				Bidirectionality Prediction			
		Cora	Citeseer	Cornell	Wisconsin	Cora	Citeseer	Cornell	Wisconsin
AP	VGAE	50.00 \pm 0.00	50.00 \pm 0.00	50.00 \pm 0.00	50.00 \pm 0.00	50.00 \pm 0.00	50.00 \pm 0.00	50.00 \pm 0.00	50.00 \pm 0.00
	HOPE	63.73 \pm 1.12	61.28 \pm 0.57	62.91 \pm 3.17	65.02 \pm 3.11	64.24 \pm 1.18	54.87 \pm 1.67	46.73 \pm 4.04	52.39 \pm 2.98
	APP	67.93 \pm 1.09	63.70 \pm 0.51	60.13 \pm 3.26	62.23 \pm 3.02	70.97 \pm 2.60	63.77 \pm 3.28	53.25 \pm 3.99	55.62 \pm 3.14
	LINE	70.26 \pm 0.76	64.08 \pm 1.11	66.87 \pm 5.78	64.39 \pm 5.32	50.25 \pm 1.01	45.49 \pm 1.62	51.13 \pm 5.89	60.61 \pm 3.68
	S/T VAE	64.62 \pm 1.37	61.02 \pm 1.37	69.80 \pm 3.82	74.64 \pm 3.68	73.86 \pm 3.04	67.05 \pm 4.10	61.65 \pm 4.22	66.33 \pm 2.73
	Gravity VAE	<u>84.50 \pm 1.24</u>	<u>79.27 \pm 1.24</u>	50.95 \pm 4.80	57.86 \pm 3.28	<u>73.87 \pm 2.82</u>	<u>71.87 \pm 3.87</u>	<u>73.03 \pm 3.78</u>	<u>69.36 \pm 3.95</u>
	MVGAE	81.07 \pm 1.52	74.33 \pm 1.61	76.37 \pm 4.56	77.08 \pm 3.47	65.01 \pm 1.28	63.26 \pm 3.07	68.23 \pm 4.29	62.88 \pm 4.01
	DiGAE	77.87 \pm 1.49	73.67 \pm 2.56	<u>73.28 \pm 4.04</u>	<u>75.06 \pm 3.75</u>	62.86 \pm 1.37	61.84 \pm 3.70	65.96 \pm 7.23	60.67 \pm 4.64
	ClusterLP	90.42 \pm 0.91	83.09 \pm 1.05	59.91 \pm 5.34	64.82 \pm 4.55	75.87 \pm 1.06	75.72 \pm 1.75	75.69 \pm 6.66	73.97 \pm 5.38
AUC	VGAE	50.00 \pm 0.00	50.00 \pm 0.00	50.00 \pm 0.00	50.00 \pm 0.00	50.00 \pm 0.00	50.00 \pm 0.00	50.00 \pm 0.00	50.00 \pm 0.00
	HOPE	61.84 \pm 1.84	60.24 \pm 0.51	65.29 \pm 3.29	69.46 \pm 3.90	65.11 \pm 1.40	52.65 \pm 3.05	57.41 \pm 3.66	61.05 \pm 3.20
	APP	69.20 \pm 0.65	64.35 \pm 0.45	64.96 \pm 3.50	66.71 \pm 3.62	72.85 \pm 1.91	64.16 \pm 1.90	64.01 \pm 4.13	62.36 \pm 3.57
	LINE	75.37 \pm 0.63	69.49 \pm 1.01	71.90 \pm 4.23	69.23 \pm 4.20	69.90 \pm 0.67	66.02 \pm 1.46	66.06 \pm 4.94	65.87 \pm 3.75
	S/T VAE	63.00 \pm 1.05	57.32 \pm 0.92	<u>72.53 \pm 4.39</u>	76.19 \pm 3.62	<u>75.20 \pm 2.62</u>	69.67 \pm 3.12	59.17 \pm 3.93	67.74 \pm 3.07
	Gravity VAE	83.33 \pm 1.11	76.19 \pm 1.35	43.73 \pm 7.17	54.57 \pm 4.07	75.00 \pm 2.10	<u>71.61 \pm 3.20</u>	69.27 \pm 4.02	68.59 \pm 3.96
	MVGAE	80.52 \pm 1.79	74.13 \pm 1.34	69.57 \pm 3.96	70.21 \pm 3.72	65.07 \pm 1.27	64.73 \pm 2.89	63.18 \pm 3.88	60.30 \pm 3.66
	DiGAE	77.08 \pm 1.49	73.53 \pm 1.97	74.79 \pm 4.01	<u>74.41 \pm 4.09</u>	62.83 \pm 1.96	60.02 \pm 3.21	62.65 \pm 4.76	57.48 \pm 4.08
	ClusterLP	89.62 \pm 0.88	81.15 \pm 1.27	56.91 \pm 7.18	64.49 \pm 5.33	75.39 \pm 1.22	73.72 \pm 1.78	71.85 \pm 6.01	73.04 \pm 4.51

Fig. 7: Changes of AUC w.r.t. different values of n .Fig. 8: Changes of AUC w.r.t. different values of β .

decays. The value of n can be judged according to the clustering coefficient of the network, a larger clustering coefficient indicates that the nodes in the network tend to create relatively closely related groups, that is, the cluster division in the network is more obvious, at this time we can set a larger n to capture this characteristic of the network, on the contrary, the cluster structure of the network is not significant and set n to a smaller value. As shown in Fig.7, increasing the value of n increases the average AUC of 10 runs when n is less than 25, while the prediction effect will decrease slightly if it continues to increase n . In general, setting n to 25 is a good choice.

- **Impact of the parameter β .** we introduced a parameter β to tune the relative importance of the node proximity w.r.t. the influence attraction, which works the same as in the undirected graph. In Fig.8, with the increase of β from 3.0 to 7.0, the values of mean AUC score are rising first and then falling when β exceeds 5.0, but a large variance accompanied. Therefore, in Table II, we will set different β values for different networks.

V. EXTENSIONS AND OPENINGS

We have presented an unsupervised graph representation learning framework which relies on leveraging cluster-level content, namely *ClusterLP*. Based on the understanding that links between nodes in the cluster are easier to form, *ClusterLP* innovatively puts forward the concept of *cluster-level proximity*, which perfectly complements the defect that *first-order proximity* cannot grasp the global information of the network. Furthermore, we propose that it can be extended to the directed graph link prediction task by simply replacing the definition of *cluster-level proximity* between nodes. Throughout these experiences, we focused on featureless graphs to fairly compete with *Node2vec* and *Gravity VAE*, etc. How to leverage node features, in addition to the graph structure summarized in A, will be the focus of our next phase of research.

REFERENCES

- [1] E. Hajiramezanali, A. Hasanzadeh, K. Narayanan, N. Duffield, M. Zhou, and X. Qian. "Variational graph recurrent neural networks," in *Advances in Neural Information Processing Systems*, pp. 10700–10710, 2019.

- [2] W. Zhang, Z. Sheng, M. Yang, Y. Li, Y. Shen, Z. Yang, and B. Cui. “NAFS: A Simple yet Tough-to-beat Baseline for Graph Representation Learning,” in *Proceedings of the 39th International Conference on Machine Learning*, pp. 26467–26483, 2022.
- [3] C. Zhou, Y. Liu, X. Liu, Z. Liu, and J. Gao. “Scalable Graph Embedding for Asymmetric Proximity,” in *Proceedings of the Thirty-First AAAI Conference on Artificial Intelligence*, San Francisco, California, USA, pp. 2942–2948, 2017.
- [4] M. Ou, P. Cui, J. Pei, and W. Zhu. “Asymmetric Transitivity Preserving Graph Embedding,” in *Proceedings of the 22nd ACM SIGKDD International Conference on Knowledge Discovery and Data Mining*, San Francisco, California, USA, pp. 1105–1114, 2016.
- [5] G. Salha, S. Limnios, and R. Hennequin. “Gravity-Inspired Graph Autoencoders for Directed Link Prediction,” in *Proceedings of the 28th ACM International Conference on Information and Knowledge Management*, Beijing, China, pp. 589–598, 2019.
- [6] G. Kollias, V. Kalantzis, T. Idé, A. Lozano, and N. Abe. “Directed Graph Auto-Encoders,” in *Proceedings of the 36th AAAI Conference on Artificial Intelligence*, vol. 36, no. 7, pp. 7211–7219, 2022.
- [7] Z. Tong, Y. Liang, C. Sun, X. Li, D. S. Rosenblum, and A. Lim. “Digraph Inception Convolutional Networks,” in *Proceedings of the 34th International Conference on Neural Information Processing Systems*, Vancouver, BC, Canada, vol.33, 2020.
- [8] G. Salha-Galvan, J. Lutzeyer, G. Dasoulas, R. Hennequin, and M. Vazirgiannis. “Modularity-aware graph autoencoders for joint community detection and link prediction,” *Neural Networks*, vol. 153, pp. 474–495, 2022.
- [9] Y. Li, Y. Wang, T. Zhang, J. Zhang, and Y. Chang. “Learning Network Embedding with Community Structural Information,” in *Proceedings of the 28th International Joint Conference on Artificial Intelligence*, Macao, China, pp. 2937–2943, 2019.
- [10] Y. Luo, A. Chen, B. Hui, and K. Yan. “Memory-Associated Differential Learning,” *arXiv:2102.05246*, 2021.
- [11] C. Mavromatis and G. Karypis. “Graph InfoClust: Maximizing Coarse-Grain Mutual Information in Graphs,” in *Advances in Knowledge Discovery and Data Mining: 25th Pacific-Asia Conference (PAKDD)*, Berlin, Heidelberg, pp. 541–553, 2021.
- [12] J. Xie, R. Girshick, and A. Farhadi. “Unsupervised deep embedding for clustering analysis,” in *Proceedings of the 33rd International Conference on Machine Learning*, New York, NY, USA, pp. 478–487, 2016.
- [13] X. Guo, L. Gao, X. Liu, and J. Yin. “Improved Deep Embedded Clustering with Local Structure Preservation,” in *Proceedings of the 26th International Joint Conference on Artificial Intelligence*, Melbourne, Australia, pp. 1753–1759, 2017.
- [14] C. Wang, S. Pan, R. Hu, G. Long, J. Jiang, and C. Zhang. “Attributed Graph Clustering: A Deep Attentional Embedding Approach,” in *Proceedings of the 28th International Joint Conference on Artificial Intelligence*, Macao, China, pp. 3670–3676, 2019.
- [15] B. Yang, X. Fu, N. Sidiropoulos, and M. Hong. “Towards K-Means-Friendly Spaces: Simultaneous Deep Learning and Clustering,” in *Proceedings of the 34th International Conference on Machine Learning*, Sydney, NSW, Australia, pp. 3861–3870, 2017.
- [16] Z. Jiang, Y. Zheng, H. Tan, B. Tang, and H. Zhou. “Variational Deep Embedding: An Unsupervised and Generative Approach to Clustering,” in *Proceedings of the 26th International Joint Conference on Artificial Intelligence*, Melbourne, Australia, pp. 1965–1972, 2017.
- [17] G. Cui, J. Zhou, C. Yang, and Z. Liu. “Adaptive Graph Encoder for Attributed Graph Embedding,” in *Proceedings of the 26th ACM SIGKDD International Conference on Knowledge Discovery & Data Mining*, Virtual Event, CA, USA, pp. 976–985, 2020.
- [18] S. Pan, R. Hu, G. Long, J. Jiang, L. Yao, and C. Zhang. “Adversarially Regularized Graph Autoencoder for Graph Embedding,” in *Proceedings of the 27th International Joint Conference on Artificial Intelligence*, Stockholm, Sweden, pp. 2609–2615, 2018.
- [19] T. Kipf and M. Welling. “Variational Graph Auto-Encoders,” *NIPS Workshop on Bayesian Deep Learning*, 2016.
- [20] A. Grover, J. Leskovec. “Node2vec: Scalable Feature Learning for Networks,” in *Proceedings of the 22nd ACM SIGKDD International Conference on Knowledge Discovery & Data Mining*, San Francisco, California, USA, pp. 855–864, 2016.
- [21] J. Tang, M. Qu, M. Wang, M. Zhang, J. Yan, and Q. Mei. “LINE: Large-Scale Information Network Embedding,” in *Proceedings of the 24th International Conference on World Wide Web*, Florence, Italy, pp. 1067–1077, 2015.
- [22] T. Yi, S. Zhang, Z. Bu, J. Du, and C. Fang. “Link prediction based on higher-order structure extraction and autoencoder learning in directed networks,” *Knowledge-Based Systems*, vol. 241, pp. 108241, 2022.
- [23] B. Wilder, E. Ewing, B. Dilkina, and M. Tambe. “End to End Learning and Optimization on Graphs,” in *Proceedings of the 33rd International Conference on Neural Information Processing Systems*, Red Hook, NY, USA, pp. 4672–4683, 2019.
- [24] Y. Zhu, Y. Xu, F. Yu, S. Wu, and L. Wang. “CAGNN: Cluster-Aware Graph Neural Networks for Unsupervised Graph Representation Learning,” *arXiv:2009.01674*, 2020.
- [25] A. R. Benson, D. F. Gleich, and J. Leskovec. “Higher-order organization of complex networks,” *Science*, vol. 353, no. 6295, pp. 163–166, 2016.
- [26] H. Ghorbanzadeh, A. Sheikhhahmadi, M. Jalili, and S. Sulaimany. “A hybrid method of link prediction in directed graphs,” *Expert Systems with Applications*, vol. 165, pp. 113896, 2021.
- [27] F. Aghabozorgi and M. R. Khayyambashi. “A new similarity measure for link prediction based on local structures in social networks,” *Physica A: Statistical Mechanics and its Applications*, vol. 501, pp. 12–23, 2018.
- [28] M. E. Newman. “Clustering and preferential attachment in growing networks,” *Physical review E*, vol. 64, no. 2, pp. 025102, 2001.
- [29] D. Liben-Nowell and J. Kleinberg. “The link-prediction problem for social networks,” *Journal of the American society for information science and technology*, vol. 58, no. 7, pp. 1019–1031, 2007.
- [30] L. A. Adamic and E. Adar. “Friends and neighbors on the web,” *Social networks*, vol. 25, no. 3, pp. 211–230, 2003.
- [31] A. Barabási and R. Albert. “Emergence of Scaling in Random Networks,” *Science*, vol. 286, no. 5439, pp. 509–512, 1999.
- [32] A. Clauset, C. Moore, and M. E. Newman. “Hierarchical structure and the prediction of missing links in networks,” *Nature*, vol. 453, no. 7191, pp. 98, 2008.
- [33] M. Al Hasan, V. Chaoji, S. Salem, and M. Zaki. “Link prediction using supervised learning,” in *SDM06: workshop on link analysis, counter-terrorism and security*, 2006.
- [34] F. Papadopoulos, M. Kitsak, M. Á. Serrano, M. Boguñá, and D. Krioukov. “Popularity versus similarity in growing networks,” *Nature*, vol. 489, no. 7417, pp. 537, 2012.
- [35] M. Girvan and M. E. J. Newman. “Community structure in social and biological networks,” *Proc Natl Acad Sci U S A*, vol. 99, no. 12, pp. 7821–7826, 2002.
- [36] B. Perozzi, R. Al-Rfou, and S. Skiena. “DeepWalk: Online Learning of Social Representations,” in *Proceedings of the 20th ACM SIGKDD International Conference on Knowledge Discovery and Data Mining*, New York, NY, USA, pp. 701–710, 2014.
- [37] Y. Lecun, L. Bottou, Y. Bengio, and P. Haffner. “Gradient-based learning applied to document recognition,” *Proceedings of the IEEE*, vol. 86, no. 11, pp. 2278–2324, 1998.